

## Magnetic susceptibility of $^3\text{He}$ at large molar volume

M. E. R. Bernier, M. Bassou, M. Chapellier, and M. Rotter\*

*Service de Physique du Solide et de Résonance Magnétique, Commissariat à l'Energie Atomique—Centre d'Etudes Nucléaires de Saclay, 91191 Gif-sur-Yvette CEDEX, France*

(Received 22 February 1989)

We report susceptibility measurements for three samples of bcc  $^3\text{He}$  at large molar volumes. The Curie-Weiss constants measured for two solid samples are in excellent agreement with the most recent values, and we do not observe the anomaly formerly reported. The melting of the solid is analyzed on the third sample.

### INTRODUCTION

Magnetic susceptibility provides useful information on the many-body phenomena in solid  $^3\text{He}$ . The Curie-Weiss constant is directly related to the atomic exchange processes, and the sign of this constant was the first indication of the antiferromagnetic tendency for spin ordering at low temperature and low magnetic field.<sup>1</sup> Measurements have been performed with increased precision in recent years, and there is a good agreement between the experiment and the theoretical model of multiple spin exchange.<sup>2-4</sup> However, for large molar volume in the bcc phase an unexpected decrease in susceptibility has been reported at low temperatures,<sup>5</sup> and various explanations have been given for this anomaly.<sup>6,7</sup> In this paper we report measurements of the magnetic susceptibility of three  $^3\text{He}$  samples, one being solid at all temperatures and two solid samples melting at low temperatures. We compare our results with recent susceptibility measurements.

### APPARATUS

Our experimental cell is made of Stycast 1266. The upper part is an open volume for the sample; the lower part is filled with packed Teflon spheres with a 2000-Å diameter (DLX 2000, manufactured by Du Pont de Nemours); and the diaphragm of a BeCu strain gauge of standard design<sup>8</sup> forms the bottom of the cell. A channel 2.5 mm in diameter open through the DLX allows the pressure to equilibrate throughout the cell.

The samples formed by the "blocked capillary" method are cooled by six silver wires with a 0.5-mm diameter, attached to a silver rod with a 6-mm diameter that is thermally anchored to the mixing chamber of a dilution refrigerator by sinter silver pellets.

The magnetic field is produced by a conventional Vari-an electromagnet, giving a maximum field of 2.5 T.

Both the temperature and the susceptibility are measured by NMR using two coils wound around the Stycast cell. A solenoid with vertical axis is wound around the He sample, and saddle coils with horizontal axis are used to observe the NMR of the fluorine spins in DLX. This signal is used as a secondary thermometer to measure the temperature of the sample. The NMR lines are recorded both in a multichannel analyzer and on a chart recorder,

and the pressure of the samples is continuously monitored. Various carbon and  $\text{RuO}_2$  resistors in the mixing chamber and on the silver rod are also used to obtain a first estimate of the temperature. A heater placed on the silver rod is used to control the temperature of the sample.

### EXPERIMENTAL PROCEDURE

We measure the susceptibility of both helium and fluorine spins in a field of 2.372 T by cw NMR, using two  $Q$  meters of frequencies  $\omega/2\pi=76.925$  MHz for helium and  $\omega/2\pi=94.9997$  MHz for fluorine. We simultaneously record the  $^3\text{He}$  and  $^{19}\text{F}$  NMR lines for each magnetic field sweep, and can measure both the height and integral of the lines. The susceptibility of the  $^{19}\text{F}$  spins has been studied at length and is known to follow a Curie law down to the millikelvin range;<sup>9,10</sup> it is an excellent secondary thermometer in good thermal contact with the sample. The signal is calibrated by comparison with the melting curve of  $^3\text{He}$  at low temperatures<sup>11</sup> where the temperature is deduced from the pressure measured with the calibrated BeCu strain gauge. The calibration is obtained at 4.2 K by measuring the pressure of a liquid- $^3\text{He}$  sample in equilibrium with a room-temperature container, where the pressure is measured by a piezoelectric transducer (Digiquartz Model 2900 AS) and a pressure transducer Sedeme CMB 50. The consistency of our pressure and temperature measurements is directly checked at low temperatures for the two samples melting at temperatures lower than the minimum of the melting curve by fitting our melting pressure versus temperature data. We also checked our pressure calibration by recording the minimum of the melting curve following the decompression of two of our samples.

Our NMR data for the three molar volumes are taken using the same  $Q$  meters with the same sensitivity so that we have a unique temperature calibration with the  $F$  spins and can make direct comparisons for the susceptibility of the three samples. We carefully choose rf levels and magnetic field sweeps to avoid the saturation of the NMR lines and any heating effect on the samples. We typically sweep the field by 23 G in 5 min. The gain of the NMR system is also checked by monitoring the output level of the  $Q$  meters and measuring the gain of the

dc amplification before and after each measurement. We also measure the characteristics of our detection to make the required corrections. As mentioned earlier, the NMR signals are recorded both on a chart recorder and by a multichannel analyzer. We can then process the digitized signals to integrate the NMR lines. All the data are reduced to normalized values of the rf injection and of the total amplification.

When the sample is formed and the capillary blocked, and before taking any data, we first anneal the solid at a temperature slightly lower than the melting temperature for at least 10 h, and then decrease the temperature slowly. We take measurements both when lowering the temperature and during warm up. After a temperature change we always wait a minimum of 6 h before taking data, allowing the sample to reach equilibrium. The data taken during the cooling down and warm up sequences are consistent.

The error for the absolute temperature is thought to be less than 3% at the lowest temperature, while the error of the susceptibility ratio is of the order 1%. When the temperature increases the error of  $T^{-1}$  in abscissa decreases, while the error on the susceptibility ratio increases due to the decrease of the NMR signals; this last feature appears clearly through the vertical scatter of the data, which is a good estimate of the overall error bars.

The molar volume of the samples is deduced from the pressure measurements using the data of Ref. 12. A last check of the molar volume is also possible for the two samples melting at low temperatures by noticing that the ratio of the melting temperatures at high and low temperatures is a monotonic function of the molar volume.

## RESULTS AND DISCUSSION

Our measurements are made on three samples of molar volumes  $V$ , 24.850, 24.574, and 24.085  $\text{cm}^3$ , respectively. Two of the samples melt at low temperatures, and we record both the pressure inside the cell and the susceptibility of the samples. We thus obtain the melting temper-

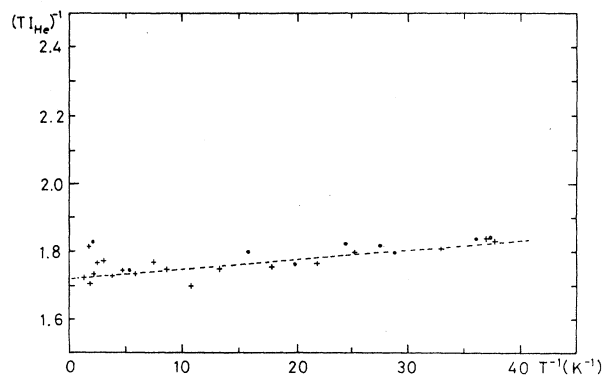


FIG. 1. The ratio of the integrals of the NMR lines of  $^{19}\text{F}$  and  $^3\text{He}$  which is proportional to  $(\chi T)^{-1}$  is plotted in arbitrary units as a function of  $T^{-1}$  at  $V=24.085 \text{ cm}^3$ . The crosses indicate data taken during the cooling down and the circles indicate data taken when warming up. The dashed straight line figures the Curie-Weiss law with  $\Theta_{\text{CW}}=1.63 \text{ mK}$ .

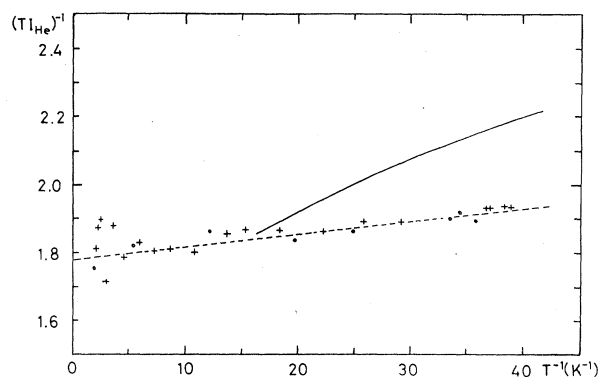


FIG. 2. The ratio of the integrals of the NMR lines of  $^{19}\text{F}$  and  $^3\text{He}$  which is proportional to  $(\chi T)^{-1}$  is plotted in the same arbitrary units as in Fig. 1 as a function of  $T^{-1}$  at  $V=24.574 \text{ cm}^3$ . The crosses indicate data taken during the cooling down and the circles indicate data taken when warming up. The dashed straight line figures the Curie-Weiss law with  $\Theta_{\text{CW}}=2.10 \text{ mK}$ . The solid line indicates the expected value of  $(\chi T)^{-1}$  for the melting of a bulk sample (see text).

ature and can correlate the susceptibility measurements to the amount of liquid formed in the cell. The third sample remains solid at low temperatures, and we deduce the Curie-Weiss temperature of this bcc solid and compare it to the existing measurements.

We reduce our data according to a procedure used in Ref. 3, i.e., we plotted  $(\chi T)^{-1}$  as a function of  $T^{-1}$ . Our measurements directly give the integrals of the  $^3\text{He}$  and  $^{19}\text{F}$  signals,  $I_{\text{He}}$  and  $I_{\text{F}}$ , two quantities proportional to the susceptibilities of He and F in our applied field, the susceptibility of F being proportional to  $T^{-1}$  in our temperature range.<sup>9,10</sup> We thus plot  $I_{\text{F}}/I_{\text{He}}$  as a function of  $I_{\text{F}}$ , i.e.,  $(T I_{\text{He}})^{-1}$  as a function of  $T^{-1}$ . The data are given in Figs. 1–3 for the three molar volumes.

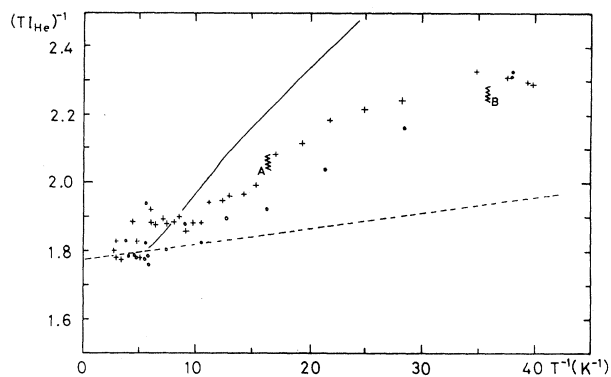


FIG. 3. The ratio of the integrals of the NMR lines of  $^{19}\text{F}$  and  $^3\text{He}$  which is proportional to  $(\chi T)^{-1}$  is plotted in the same arbitrary units as in Figs. 1 and 2 as a function of  $T^{-1}$  at  $V=24.850 \text{ cm}^3$ . The crosses indicate data taken during the cooling down and the circles indicate data taken when warming up. The points A and B give the temperatures where the capillary plug moved during this run. The dashed straight line figures the expected Curie-Weiss law for the solid sample using a value of the Curie-Weiss temperature extrapolated from the best measurements (Refs. 2 and 3); the solid line indicates the expected value of  $(\chi T)^{-1}$  for the melting of a bulk sample, ignoring any confined geometry effect (see text).

(1) The sample  $V=24.085 \text{ cm}^3$  is solid in the whole temperature range. The curve  $(TI_{\text{He}})^{-1}=f(T^{-1})$  is a straight line as expected and  $\Theta_{\text{CW}}=1.63 \text{ mK}$  in good agreement with the most recent measurements<sup>2-4</sup> (Fig. 1).

The sensitivity of our system is unchanged for the three studied molar volumes. Since  $(TI_{\text{He}})^{-1}$  is proportional to the inverse susceptibility of  $^3\text{He}$ , i.e., to  $V$ , the knowledge of this quantity extrapolated at infinite temperature is useful to reduce the data of the other two molar volumes where the solid exists only in a smaller temperature range, making the extrapolation less precise.

(2) The data for  $V=24.850 \text{ cm}^3$  are plotted in Figs. 3 and 4. The solid melts at low temperatures at a constant volume, and the susceptibility exhibits a decrease due to the lower susceptibility of the liquid phase. Using the pressure measurements, we know the melting temperature of the sample, and we can calculate the amount of liquid formed along the melting curve and the expected susceptibility of the mixture obtained at low temperatures, using the data of references.<sup>13,14</sup> This curve is plotted as a solid line in Fig. 3. We also plotted the straight line figuring the susceptibility of a sample of the same molar volume assuming it does not melt at low temperatures.

It is worth mentioning the history of this sample,  $V=24.850 \text{ cm}^3$ , which is close to the minimum of the melting curve. Before taking data, the sample was cycled a first time to the lowest temperature, then warmed up to 380 mK for several days. During the run where the data were taken, and after melting the solid at low temperatures, the plug of solid in the capillary slipped a first time in *A* when cooling down and a second time later in *B* during the warm up. In both cases the plug slid towards the outside, slightly decreasing the pressure in the cell. Both effects were small and did not change much the number of spins in the cell, i.e., the susceptibility, but they could be seen on the pressure gauge.

We notice at once, that while the susceptibility de-

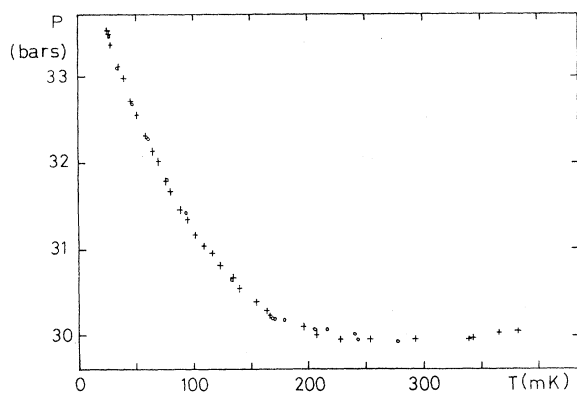


FIG. 4. The pressure inside the constant volume cell is plotted as a function of temperature for a solid sample of molar volume  $V=24.850 \text{ cm}^3$  melting at low temperature. The crosses are data taken during the cooling down, the circles are data taken during the warm up.

creases as expected due to the melting of the sample, the change of susceptibility is smaller than expected from the calculated fraction of liquid formed in the cell. However, the NMR coil placed in the upper part of the cell can only see the solid-liquid mixture in the open volume but not the helium embedded between the DLX Teflon spheres (of 2000 Å diameter), which occupy roughly 25% of the total volume of the cell. It is well known that confined geometries with typical sizes of the order of 100 Å displace the melting curve of  $^4\text{He}$ ,<sup>15,16</sup> and the same is expected for  $^3\text{He}$ .<sup>16</sup> This type of behavior is confirmed by a slight rounding off of the  $P(T)$  data before reaching the melting curve when cooling down, as appears in Fig. 4. In our case, it would make the first liquid appear around the DLX spheres thus changing, slightly, the pressure of the rest of the sample and also the ratio of liquid to solid to be formed in the open volume. It can be shown (Appendix) that within crude but simple assumptions the fraction of liquid missing in the open volume is proportional to the fraction of liquid formed in the DLX. This implies that a fraction of the liquid will not be observed while decreasing the temperature along the melting curve, this fraction increasing when the temperature decreases to reach a limiting value corresponding to the filling of the space between the spheres by liquid. At 30 mK our susceptibility measurement corresponds to a fraction of 20% of the liquid in the NMR coil, while we would expect 35% of the liquid for an open geometry cell. The formation of liquid in the NMR coil is also noticeable when we plot the amplitude versus the integral of the NMR signal. Such a plot is a straight line for a solid sample but deviates from a linear function as the liquid is not homogeneously formed in the open volume. In our cell, the integral of the line grows significantly slower than the amplitude as the temperature decreases below 80 mK. (Our sample melts close to 180 mK.)

Taking into account the preceding limitations, we observe no drastic decrease of the susceptibility of the solid unless it would be more than compensated by the tendency of liquid to appear around the DLX spheres.

(3) The data for  $V=24.574 \text{ cm}^3$  are plotted in Figs. 2 and 5. The pressure measurements indicate that the solid melts at  $T \sim 75 \text{ mK}$  when reaching the lowest part of the melting curve, but the NMR susceptibility curve does not indicate any melting of the bulk part of the sample in the NMR coil. The amplitude of the NMR signal also remains a linear function of the integral, with the same slope as obtained for the solid sample at  $V=24.085 \text{ cm}^3$  and the high-temperature data (solid) at  $V=24.850 \text{ cm}^3$ . If not an absolute proof, this fact is consistent with a bulk sample remaining solid in the open volume of the NMR coil. This can be understood by the preceding analysis of the melting in our cell. This sample was formed and annealed at high temperatures but was not cycled to the lowest temperature before taking data. For a bulk sample of the same molar volume 16% of the liquid would be formed along the melting curve when reaching our lowest temperature but as we expect most of it to be formed around the DLX spheres, no significant amount of melting can be seen in the open volume. From Fig. 2 we then deduce the Curie-Weiss temperature for a solid sample of

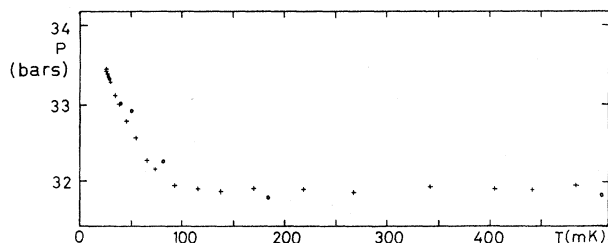


FIG. 5. The pressure inside the constant volume cell is plotted as a function of temperature for a solid sample of molar volume  $V=24.574 \text{ cm}^3$  melting at low temperature. The crosses are data taken during the cooling down, the circles are data taken during the warm up.

molar volume  $V=24.574 \text{ cm}^3$ ,  $\Theta_{\text{CW}}=2.10 \text{ mK}$ , a value in good agreement with the extrapolation of the most precise measurements.<sup>2,3</sup> We must point out that the molar volume changes slightly at the lowest temperature when the liquid is formed in the DLX spheres.

Within the precision of our measurements we observe no anomalous susceptibility for the solid down to our lowest temperature ( $T \sim 26 \text{ mK}$ ).

### CONCLUSION

We report the measurements of susceptibility for three solid  $^3\text{He}$  samples of large molar volume. One sample is expected to remain solid down to zero temperature, a second one remains solid but would melt by further lowering the temperature, the last one melts in the temperature range of our measurements. The Curie-Weiss constant of the two solid samples is in excellent agreement with the most precise measurements and the susceptibility for the sample  $V=24.574 \text{ cm}^3$ , in a molar volume range where an anomaly was reported earlier, is not anomalous. The sample melting at low temperatures shows a decrease of susceptibility due to the appearance of liquid in the cell but the amount of liquid observed is lower than expected for an open geometry, a fact attributed to the presence of DLX spheres of  $2000 \text{ \AA}$  in diameter, acting as a volume of confined geometry, which displaces the melting curve and where the liquid formed in the cell appears preferentially.

### ACKNOWLEDGMENTS

It is a pleasure to acknowledge the most valuable technical assistance of Mr. G. Guerrier.

### APPENDIX: MELTING OF A SAMPLE OF SOLID HELIUM AT CONSTANT VOLUME

Let us consider a constant-volume cell with both open and confined geometry parts. We assume that the equilibrium liquid  $v_{l_1}$  and solid  $v_{s_1}$  molar volumes along the melting curve, which are well known for bulk samples, are displaced to  $v_{l_2}$  and  $v_{s_2}$  in confined geometries, corresponding to a displacement of the melting curve towards higher pressures at constant temperature as known for solid  $^4\text{He}$  (Refs. 15 and 16) and expected for solid  $^3\text{He}$ .<sup>16</sup> This is a crude approximation as the melting curve is probably displaced by various amounts depending on the characteristic dimensions of the confined geometry. When a solid sample is cooled down it first crosses the melting curve for confined geometry and forms liquid, the pressure changes slightly in the cell. At constant temperature the volume change due to the melting of  $n_{l_2}$  moles of solid in the confined geometry is  $n_{l_2}(v_{l_2} - v_{s_2})$ . As the volume of the cell is constant, the molar volume of the remaining solid changes. When the confined geometry is filled with liquid, the conservation of the number of atoms and of the volume gives

$$n_{l_1} = \frac{v_0 - v_{s_1}}{v_{l_1} - v_{s_1}} - n_{l_2} \frac{v_{l_2} - v_{s_1}}{v_{l_1} - v_{s_1}},$$

where  $v_0$  is the molar volume of the starting solid and  $n_{l_1}$  the number of moles of liquid formed in the open geometry. The quantity  $v_{l_2} - v_{s_1}$  is expected to be smaller than  $v_{l_1} - v_{s_1}$  by a significant factor,<sup>15</sup> and consequently the amount of liquid observed in the NMR coil is reduced by a fraction of the liquid formed in the confined geometry.

As a last point, let us mention that the liquid formed in the confined geometry can nucleate the melting of the solid in contact with it and avoid any supercooling of bulk solid in its vicinity.

\*Permanent address: Charles University, Prague, Czechoslovakia.

<sup>1</sup>W. P. Kirk, E. B. Osgood, and L. Garber, Phys. Rev. Lett. **23**, 833 (1969).

<sup>2</sup>C. T. Van Degrift, W. J. Bowers, Jr., P. B. Pipes, and D. F. McQueeney, Phys. Rev. Lett. **49**, 149 (1982).

<sup>3</sup>W. P. Kirk, Z. Olejniczak, P. Kobiela, A. A. V. Gibson, and A. Czermak, Phys. Rev. Lett. **51**, 2128 (1983).

<sup>4</sup>M. E. R. Bernier, E. Suaudeau, and M. Roger, Phys. Rev. B **38**, 737 (1988).

<sup>5</sup>W. P. Kirk, Z. Olejniczak, P. S. Kobiela, and A. A. V. Gibson, in *Proceedings of the 17th International Conference on Low Temperature Physics, LT17, Karlsruhe, 1984*, edited by U. Eckern *et al.* (Elsevier, British Vancouver, 1984), p. 273.

<sup>6</sup>P. Kumar and N. S. Sullivan, Phys. Rev. Lett. **55**, 963 (1985); Phys. Rev. B **35**, 3162 (1987).

<sup>7</sup>M. E. R. Bernier and E. Suaudeau, Phys. Rev. B **38**, 784 (1988).

<sup>8</sup>G. C. Straty and E. D. Adams, Rev. Sci. Instrum. **40**, 1393 (1969).

<sup>9</sup>P. C. Hammel, Ph.D. thesis, Cornell University, 1984; P. C. Hammel, M. L. Roukes, Y. Hu, T. J. Gramila, T. Mamiya, and R. C. Richardson, Phys. Rev. Lett. **51**, 2124 (1983).

<sup>10</sup>A. Schuhl, Thèse d'Etat, University Paris-Sud, 1986.

<sup>11</sup>D. S. Greywall, Phys. Rev. B **33**, 7520 (1986).

<sup>12</sup>S. B. Trickey, W. P. Kirk, and E. D. Adams, Rev. Mod. Phys. **44**, 668 (1972).

<sup>13</sup>H. Ramm, P. Pedroni, J. R. Thomson, and H. Meyer, J. Low Temp. Phys. **2**, 539 (1970).

- <sup>14</sup>J. C. Wheatley, *Rev. Mod. Phys.* **47**, 415 (1975).
- <sup>15</sup>E. D. Adams, K. Uhlic, Yi-Hua Tang, and G. E. Haas, *Phys. Rev. Lett.* **52**, 2249 (1984); in *Proceedings of the 17th International Conference on Low Temperature Physics, LT17, Karlsruhe, 1984*, edited by U. Eckern *et al.* (Elsevier, British Vancouver, 1984), p. 514.
- <sup>16</sup>A. L. Thomson, D. F. Brewer, S. R. Haynes, *Proceedings of the 17th International Conference on Low Temperature Physics, LT17, Karlsruhe, 1984*, edited by U. Eckern, *et al.* (Elsevier, British Vancouver, 1984).